

# Electrostatic probe disruption of drift waves in magnetized microdischarges

Cite as: Appl. Phys. Lett. **94**, 211501 (2009); <https://doi.org/10.1063/1.3132587>

Submitted: 12 March 2009 . Accepted: 21 April 2009 . Published Online: 27 May 2009

T. Ito, and M. A. Cappelli



View Online



Export Citation

## ARTICLES YOU MAY BE INTERESTED IN

[Self-organization in planar magnetron microdischarge plasmas](#)

Applied Physics Letters **106**, 254104 (2015); <https://doi.org/10.1063/1.4922898>

[Cross-field electron transport induced by a rotating spoke in a cylindrical Hall thruster](#)

Physics of Plasmas **19**, 013503 (2012); <https://doi.org/10.1063/1.3671920>

[Transition in electron transport in a cylindrical Hall thruster](#)

Applied Physics Letters **97**, 091501 (2010); <https://doi.org/10.1063/1.3486164>



## Your Qubits. Measured.

Meet the next generation of quantum analyzers

- Readout for up to 64 qubits
- Operation at up to 8.5 GHz, mixer-calibration-free
- Signal optimization with minimal latency

Find out more



# Electrostatic probe disruption of drift waves in magnetized microdischarges

T. Ito<sup>1</sup> and M. A. Cappelli<sup>2,a)</sup>

<sup>1</sup>Frontier Research Base for Global Young Researchers, Frontier Research Center, Graduate School of Engineering, Osaka University, 2-1 Yamadaoka, Suita, Osaka 565-0871, Japan

<sup>2</sup>Department of Mechanical Engineering, High Temperature Gasdynamics Laboratory, Stanford University, Stanford, California 94305-3032, USA

(Received 12 March 2009; accepted 21 April 2009; published online 27 May 2009)

Ultrahigh speed images of  $\mathbf{E} \times \mathbf{B}$  discharges are collected during electrostatic probing of magnetized microdischarges. Two azimuthally separated floating micro-Langmuir probes inserted into an axisymmetric microscale magnetically confined plasma are used to characterize azimuthal drift waves. The images reveal features associated with probe intrusion, showing how the electrostatic probes may disrupt the otherwise coherent azimuthal waves. The resulting wave dispersion calculated from the probe signals is consistent with the disruptions seen in the images. These images demonstrate how probe measurements of fluctuations and turbulence, even when probe dimensions are much smaller than characteristic discharge scales, must be interpreted with caution. © 2009 American Institute of Physics. [DOI: 10.1063/1.3132587]

The study of fluctuations in plasmas continues to be an active area of research. Correlated fluctuations in plasma density and electric field can cause anomalous transport of particles across magnetic flux surfaces. The understanding of the turbulent behavior of laboratory plasmas often depend on the use of Langmuir probes, as these probes afford the spatial resolution that is not available with microwave-based measurements. While it is well known that biased and even floating probes can perturb the nature of the plasma in the probe's vicinity, probes are used nonetheless because of their convenience and because of a lack of alternative measurements, particularly for plasmas of small scales ( $<1$  cm). As a result, probe-based measurements of time-average properties in quiescent plasmas, as well as fluctuating properties from cross correlation between multiple probes in fluctuating plasmas, are often presented without question about reliability or interpretation of the data.

In this letter, we present Langmuir probe studies of fluctuations in a microdischarge generated in a dipole magnetic field. We have used these discharges as microion sources<sup>1</sup> and as micropropulsion devices.<sup>2</sup> Others<sup>3</sup> have used similar discharges in applications related to silicon etching. Under the conditions described in Refs. 1 and 2, the xenon ions gain  $>100$  eV of directed energy and are not magnetized (i.e., their Larmor radius  $\gg$  discharge scale length). Using ultrahigh speed imaging of the plasma through a transparent anode, we have shown<sup>4</sup> that relatively strong and coherent fluctuations can be excited in these microdischarges, particularly when operating on argon and at modest pressure ( $\sim 20$  Pa). The lower resulting ion energy and the use of a lighter atom such as argon reduces the Larmor radius so that it is of comparable scale to the strong magnetic field region. Under these conditions, we expect a moderate ion temperature that is partially confined by the magnetic field and that exhibits instabilities characteristic of magnetized plasmas when subject to strong property gradients. The imaging revealed that this particular plasma exhibits large-scale disturbances in emission of relatively low mode number ( $m \leq 5$ ) that propagate along

the negative  $\mathbf{E} \times \mathbf{B}$  (azimuthal) direction, likely due to fluctuations in plasma density, which we attribute to drift waves driven by density gradients,  $\nabla n$ . The plasma also exhibits finer scale features at higher frequencies that may not be easily resolved by the imaging.

To characterize the higher frequency and shorter wave-number disturbances that cannot be resolved by our emission studies,<sup>4</sup> we introduced two azimuthally separated floating Langmuir probes. Ultrahigh speed imaging of the plasma taken during probe collection reveals information about the possible intrusive nature of these probes, raising questions about the validity of probe measurements on these and similar discharges in studying wave propagation. Under some conditions—where coherent waves are seen by imaging in the absence of the probes—the insertion of the probes resulted in a broader wave dispersion and also spectrally broadened the discharge current fluctuations.

A schematic of this discharge and experimental arrangement, as well as a photograph as seen from the side, is shown in Fig. 1. The direct-current magnetized microdischarge plasma is generated between two parallel electrodes compris-

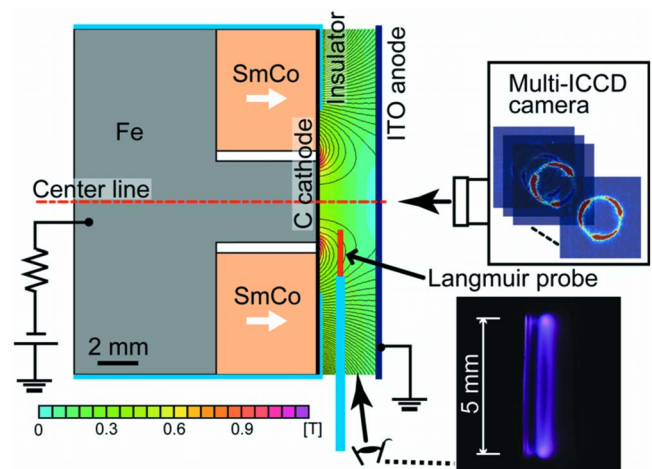


FIG. 1. (Color online) Schematic diagram of the experimental setup of the magnetized microdischarge plasma source, and photograph (side view) of the discharge operating on argon.

<sup>a)</sup>Electronic mail: cap@stanford.edu.

ing a graphite-coated cathode and an indium tin oxide (ITO) anode. The discharge voltage  $\phi_d$  and gap  $d$  are variable, but for the results presented in this paper are at nominally 280 V and 2.8 mm, respectively, for an average electric field of  $E = 10^5$  V/m. The discharge chamber is maintained at an argon pressure of 20 Pa (0.15 Torr), resulting in  $E/n \approx 2 \times 10^{-17}$  V m<sup>2</sup> ( $2 \times 10^4$  Td). The cathode covers the magnetic circuit, which consists of a ring-shaped SmCo permanent magnet and an iron core for field shaping. The outer diameter of the magnet is 17 mm, the inner diameter is 5 mm, and the thickness is 5 mm. The outer diameter of the iron core inside the magnet is 4 mm. The total thickness of the graphite-coated cathode is approximately 120  $\mu$ m. The probes consist of silver-coated copper wires, 250  $\mu$ m in diameter, located approximately midway between the electrodes, extending in from the side to about the region between the inner (iron) and outer (SmCo) poles and separated along the azimuthal direction by approximately 2 mm. The time-resolved floating potentials from each probe are recorded on a digital oscilloscope. We understand that a probe diameter of approximately 1/10th the discharge gap size may be too large to confidently probe such a microscale plasma, but these early studies required probes sufficiently rigid for accurate positioning. Future studies will be carried out with probes of varying sizes, smaller in diameter.

The magnetic dipole field generated by this structure is simulated using a commercially available finite element-based field solver.<sup>5</sup> The results for the computed field are also shown in Fig. 1. The magnetic field has a toroidal geometry, uniform in the azimuthal direction, but varying between the cathode and anode (along the radial  $r$  and axial  $z$  direction), and is strongest near the region between the iron core and magnet. The maximum field strength in this region is approximately 1 T. Given that the ions will have an average energy  $\bar{\epsilon} \approx E\lambda = (E/n)/\sigma_{cx}$ , then at this magnetic field and using a charge exchange cross-section of  $5 \times 10^{-19}$  m<sup>2</sup>,<sup>6</sup> we expect that they will have an average energy of about 40 eV and a Larmor radius of approximately 5 mm, i.e., comparable to the electrode spacing.

High speed images are obtained through the ITO anode with an ultrahigh framing rate camera (Cordin, model 222C-16UV), which has eight individual intensified charge coupled device arrays. The eight cameras can be triggered in sequence with a delay between frames to within nanoseconds. At a framing rate of 330 kHz or lower, a series of 16 equally spaced images of the plasma can be obtained (each of the eight arrays capable of acquiring two images separated by 3  $\mu$ s). At higher frame rates, we can take two sequential eight-frame movies, each of which have framing rates of greater than 330 kHz, but separated by a minimum of 3  $\mu$ s. The use of this high speed camera allows us to observe the self-organized dynamical behavior of this discharge.

Figure 2(a) shows a sequence of four images of the unfiltered emission from the discharge operating at 277 V and 9.3 mA, taken without the presence of the floating Langmuir probes within the toroidal plasma. The images are 1  $\mu$ s apart, with a single frame integration time (gate width) of 0.75  $\mu$ s. The images, which span a field of  $9.6 \times 9.6$  mm<sup>2</sup>, contain a total of  $1.5 \times 10^5$  pixels. The remaining four images captured by the camera (not shown) are a consistent spatial-temporal continuation of the features shown in this frame set. Post processing is used to smooth the images over

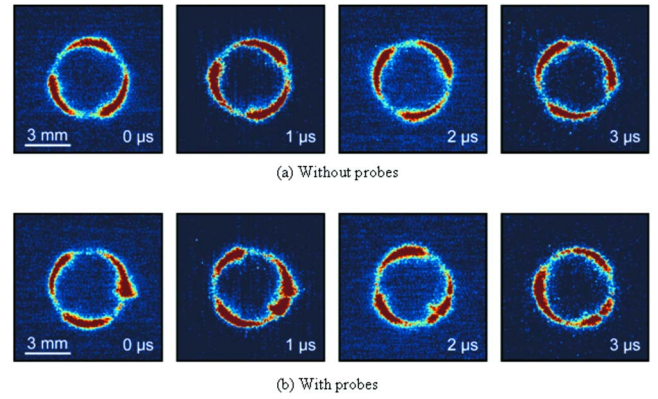


FIG. 2. (Color online) Images taken of the magnetized argon plasma (277 V and 9.3 mA). The gate width of the intensifiers is 0.75  $\mu$ s. (a) Without the probes in position. (b) With the probes in position.

the nearest neighboring pixels (nine-pixel smoothing), to remove pixel-to-pixel variations in sensitivity, resulting in a limiting spatial resolution of approximately 40  $\mu$ m. The image sequence clearly reveals the presence of a very organized coherent  $m=3$  azimuthal sinusoidal disturbance that is found to be propagating in the *negative*  $\mathbf{E} \times \mathbf{B}$  direction. The wavelength is approximately  $\lambda=5$  mm, and any single wave makes a complete revolution around the azimuth in approximately 16  $\mu$ s, corresponding to a phase velocity of  $10^3$  m/s and a frequency of  $f=0.2$  MHz. Such a dispersion is consistent with drift-wave instabilities driven by magnetized plasmas of electron temperatures of  $O(10$  eV) and density gradients scale lengths  $L_{\nabla n} = [(1/n)\nabla n]^{-1} \approx 10^{-3}$  m.<sup>7</sup> Varying operating conditions can lead to variations in the mode number of these azimuthal disturbances, with some cases as high as  $m=5$ .<sup>8</sup> While the mechanism that excites these waves is not yet well understood, we suspect that they may be driven by strong oscillations seen in the discharge current at these same frequencies, which we attribute to ionization instabilities.

Figure 2(b) shows a similar sequence of four images of the emission, but this time, with the probes inserted in the discharge. The probes are located at an angle of approximately  $120^\circ$  and  $140^\circ$  on these figures, with their position coincident with an apparent interruption in the discharge emission. While the general features of the  $m=3$  mode are preserved over much of the annular discharge, there is a clear degradation of the mode in the vicinity of the probes. In particular, the region between the probes shows a persistent emission independent of the phase of the disturbances, suggesting that there may be current flow between the probes and there is an enhancement in the emission at the wave front. We surmise that this probe disturbance will lead to degradation in the wave dispersion that is determined from the cross correlation between the two probe signals.

A wavelet decomposition analysis is carried out on the two probe signals to obtain the wave dispersion characteristics. The power spectral density resulting from this analysis is presented in Fig. 3. While the wave dispersion obtained from the probes reproduces an expected contribution from the dominant wavenumber and frequency depicted in the images (in the absence of the probes) at  $2 \times 10^2$  m<sup>-1</sup> and 0.2 MHz, respectively, it is apparent that the Langmuir probe measurements indicate the presence of a spectrally broadened disturbance of approximately constant phase velocity

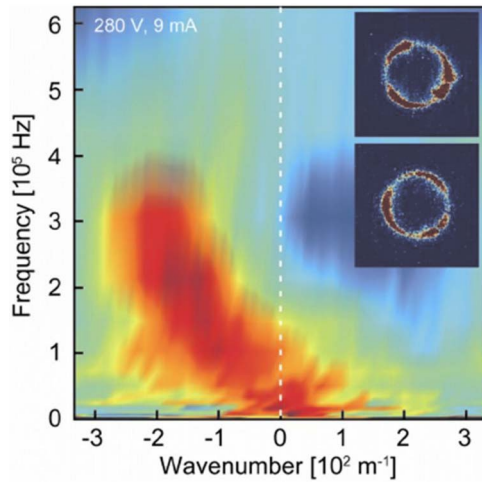


FIG. 3. (Color online) Wave dispersion map for the 280 V case derived from the azimuthally spaced electrostatic probes. The inset shows two images from the high speed emission studies.

extended over a range of wavenumber—a feature inconsistent with the high speed emission measurements. While it is possible that the emission seen by the high speed camera may not be an accurate reflection of either the plasma density or plasma potential fluctuations, an examination of the discharge current fluctuations seen with and without the presence of the probes (see Fig. 4) confirms that these probes dramatically change the nature of the current fluctuations. We conjecture that the increased discharge current seen in Fig. 4 originates from the perturbed plasma in the immediate vicinity of the probes, as the images reveal that the other regions around the annulus remain relatively unperturbed. It seems, then, that the intrusive nature of the probes is highly localized for the conditions presented here, but has strong overall impact on the discharge current fluctuations.

The discharge can be operated at slightly lower voltage, 264 V, where, under these conditions, high speed imaging indicates the presence of azimuthal disturbances with  $m=3$  or 4 mode propagation. Images taken with the presence of the probes under these conditions reveal the persistence of

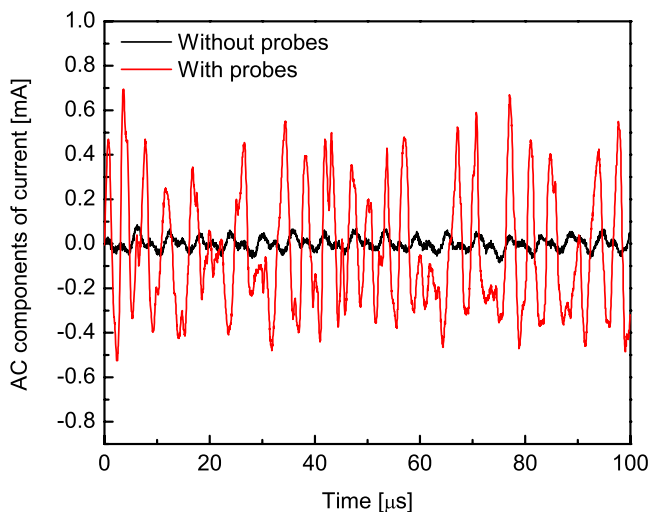


FIG. 4. (Color online) Oscillogram of the oscillating component of the discharge current (280 V). The black (solid) line corresponds to the case without the electrostatic probes while the red (dashed) line is when the probes are present.

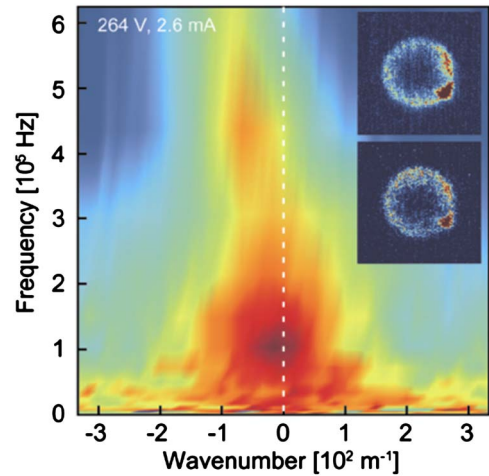


FIG. 5. (Color online) Wave dispersion map for the 264 V case derived from the azimuthally spaced electrostatic probes. The inset shows two images from the high speed emission studies.

strong emission between the two probes (see inset of Fig. 5), and a corresponding dispersion map (Fig. 5) that is consistent with the images, depicting the presence of a relatively strong, long wavelength disturbance of high phase velocity. The features in this map are likely to be artifacts of the probe intrusion. The greater perturbation introduced by the probes at this condition is attributed to the movement of the denser plasma density region toward the plane occupied by the probes as the discharge voltage is reduced.<sup>8</sup> At the higher discharge voltage condition of Fig. 4, the discharge seems to be most dense very near the cathode, and the probes are barely immersed in the highest density region.

While under some conditions in these microcharges we see that electrostatic probes can provide information that reflects the nature of drift wave propagation—even under the best of conditions, it appears that the results are to be interpreted as qualitative, at best. The probes in these studies were placed close to each other to resolve the principal azimuthal modes as identified by high speed imaging, and the images suggest that the interferences to the plasma may be caused by the relative proximity of these probes. While these intrusive probes have deficiencies from a diagnostic standpoint, they do provide opportunities for control of coherent fluctuations, and, therefore, control of transport. Future experiments will investigate this, and also if single probes or multiple probes placed further apart have similar effects on the discharge current and emission.

This research was supported by the NSF under Grant No. DE-FG02-06ER54897. Support for T. Ito is provided by the FRBGYR, through the Promotion of Environmental Improvement to Enhance Young Researchers' Independence.

<sup>1</sup>T. Ito and M. A. Cappelli, *Appl. Phys. Lett.* **89**, 061501 (2006).

<sup>2</sup>T. Ito, N. Gascon, W. S. Crawford, and M. A. Cappelli, *J. Propul. Power* **23**, 1068 (2007).

<sup>3</sup>C. G. Wilson and Y. B. Gianchandani, *IEEE Trans. Plasma Sci.* **32**, 282 (2004).

<sup>4</sup>T. Ito and M. A. Cappelli, *IEEE Trans. Plasma Sci.* **36**, 1228 (2008).

<sup>5</sup>D. C. Meeker, Finite Element Method Magnetics, Version 4.0 (<http://femm.foster-miller.net>).

<sup>6</sup>A. V. Phelps, *J. Appl. Phys.* **76**, 747 (1994).

<sup>7</sup>T. H. Stix, *Waves in Plasmas* (Springer, New York, 1992), p. 64.

<sup>8</sup>T. Ito and M. A. Cappelli, Proceedings of the Fundamentals and Applications of Microplasmas, San Diego, CA, 1–6 March 2009 (unpublished).